Supplementary Information

Coated Sulfated Zircona/SAPO-34 for the direct conversion of CO_2 to light olefins

Authors: *Adrian Ramirez[a], Abhishek Dutta Chowdhury[a], Mustafa Caglayan[a], Alberto Rodriguez-Gomez[a], Nimer Wehbe[b], Edy Abou-Hamad[b], Lieven Gevers[a], Samy Ould-Chikh[a], and Jorge Gascon[a*]*

[a]King Abdullah University of Science and Technology, KAUST Catalysis Center (KCC), Advanced Catalytic Materials, Thuwal 23955, Saudi Arabia.

[b]King Abdullah University of Science and Technology, Core Labs, Thuwal 23955, Saudi Arabia.

Correspondence to: jorge.gascon@kaust.edu.sa

INDEX:

Table S1. Comparison of the state of the art bifunctional catalyst for the CO_2 hydrogenation towards light olefins.

Catalyst	Temp (ºC)	P (bar)	GHSV (ml/h/gcat)	Conv (%)	Sel[a] CO (%)	Sel[a] C_1 (%)	Sel[a] C_2-C_4= (%)	$STY_{C2-C4=}$ (mmol/g_{cat}/h)	Ref[c]
In_2O_3-ZrO_2/SAPO-34	400	30	9000	36	85	1	12	4.1	9
In_2O_3-ZrO_2/SAPO-34	400	15	12000	22	90	1	9	2.6	15
$ZnGa_2O_4$/SAPO-34	370	30	5400	13	49	N/A[b]	46	3.6	16
In_2O_3-ZrO_2/SAPO-34	400	30	9000	36	85	1	12	4.1	17
InZr/SAPO-34	380	30	9000	26	64	1	27	7.1	18
$ZnZrO_2$/Zn-SAPO-34	380	20	3600	21	27	10	51	4.2	19
Fe_2O_3-KO_2/MOR[d]	375	30	5000	48	14	16	34	9.2	14
CuZnZr/Zn-SAPO-34	400	20	3000	20	59	6	25	1.6	20
In2O3-ZrO2/SAPO-5	300	30	4000	7	56	3	32	1.0	21
ZnO-Y2O3/SAPO-34	390	40	1800	28	85	0.3	13	0.7	22
In_2O_3-ZrO_2/SAPO-34	380	30	9000	17	55	0.7	37	6.1	46
ZnZrO2@Al2O3/SAPO-34	380	30	3500	21	45	1.3	41	3.4	47

[a] **Total product selectivity.**
[b] **Data not available.**
[c] **Main text reference.**
[d] **Without CO cofeeding.**

Table S2: Surface area (BET) and micropore analysis of SAPO-34 and Zr/SAPO-34.

	S_{BET} (m^2/g)	S_{micro}* (m^2/g)	V_{total}** (ml/g)	V_{micro}*** (ml/g)
SAPO-34	770	762	0.28	0.27
ZrS/SAPO-34	511	496	0.2	0.18

*** $S_{micro} = S_{BET} - S_{meso/ex}$**

**** Single point adsorption total pore volume @ p/p^o=0.95**

***** From N_2 adsorption isotherm using the t-plot method**

Table S3: Acidity quantification from NH_3 TPD of the SAPO-34 and ZrS/SAPO-34 materials.

	NH_3 desorbed/mass (µmol/g)	**NH_3 desorbed/ SBET (µmol/m2)**
SAPO-34	666.33	0.865
ZrS/SAPO-34	430.01	0.842
ZrS/SAPO-34-Water treatment	589.88	1.154

Table S4: Mass yield (%) to the different C_2-C_5 olefins obtained in the 1-Octene cracking experiments for the SAPO-34 and ZrS/SAPO-34 materials after 2 hours on the stream.

		Olefin mass yield (%)				
	WATER	C2=	C3=	C4=	C5=	SUM
SAPO-34	YES	0.04	0.22	0.27	0.21	0.73
ZrS/SAPO-34	YES	0.04	0.25	0.53	0.42	1.23
SAPO-34	NO	0.04	0.11	0.02	0.02	0.19
ZrS/SAPO-34	NO	0.06	0.08	0.01	0.06	0.21

Table S5: Product distribution of control experiment with Ethylene co-fed with ^{13}CO on SAPO-34 after 2 hours on the reaction stream.

Sel C_1 (%)	**Sel C_2 (%)**	**Sel C_3 (%)**	**Sel $C_{3=}$ (%)**	**Sel C_4 (%)**	**Sel $C_{4=}$ (%)**	**Sel C_5 (%)**	**Sel $C_{5=}$ (%)**	**Sel C_6 (%)**	**Sel $C_{6=}$ (%)**
1.82	13.93	26.26	34.87	2.31	7.17	1.23	8.48	0.35	3.63

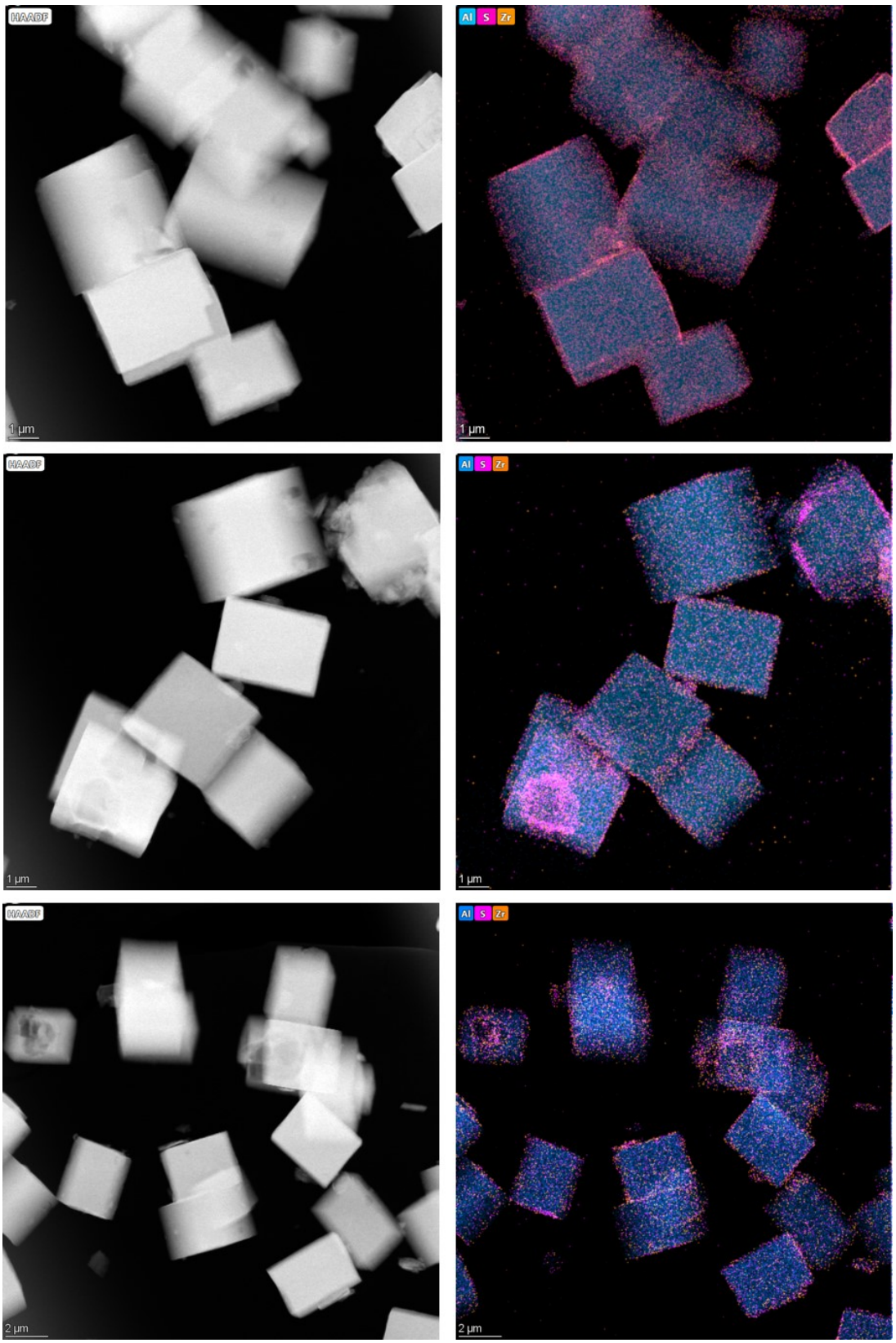

Figure S1. HAADF-STEM images of the ZrS/SAPO-34 material showing several coated particles.

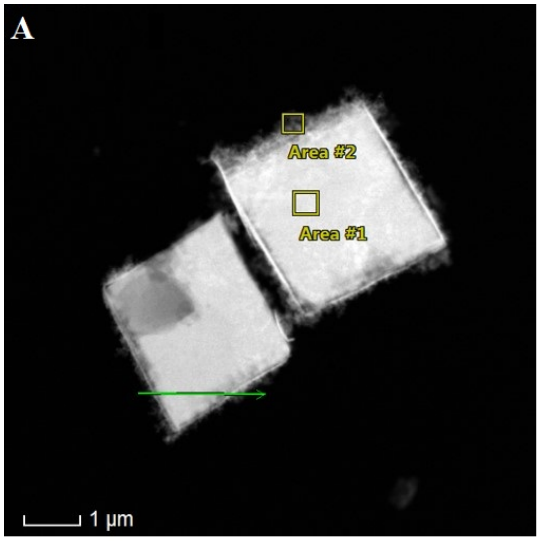

B

Element	Area 1	Area 2
	Mass fraction (%)	
O	36.2	42.1
Al	31.1	20.7
Si	4.2	1.6
P	26.8	16.2
S	0.5	5.1
Zr	1.2	14.4

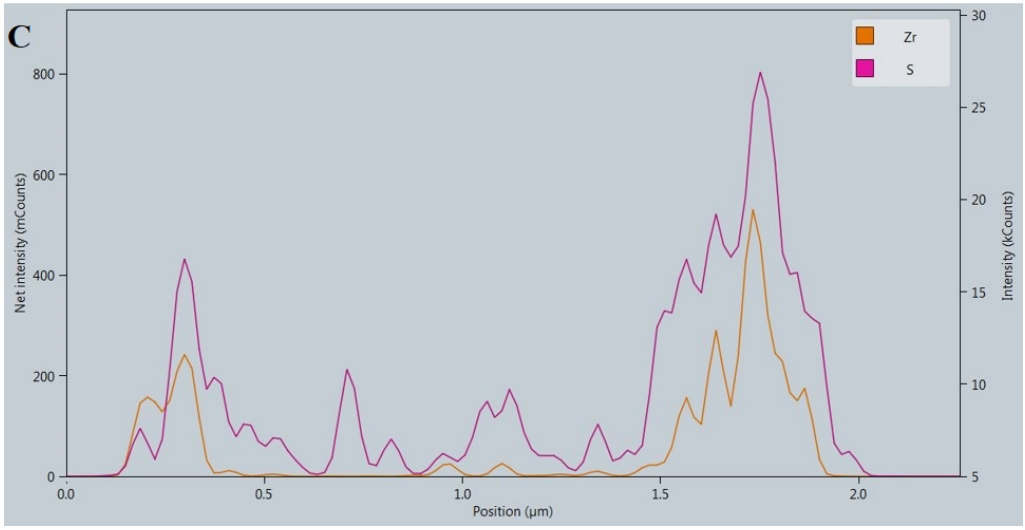

Figure S2. HAADF-STEM elemental analysis of the ZrS/SAPO-34. (A) HAADF-TEM image of the ZrS/SAPO-34. (B) Elemental composition of the areas in the yellow boxes of Figure S1.A. (C) Zr and S elemental profile alongside the gree line of Figure S1.A.

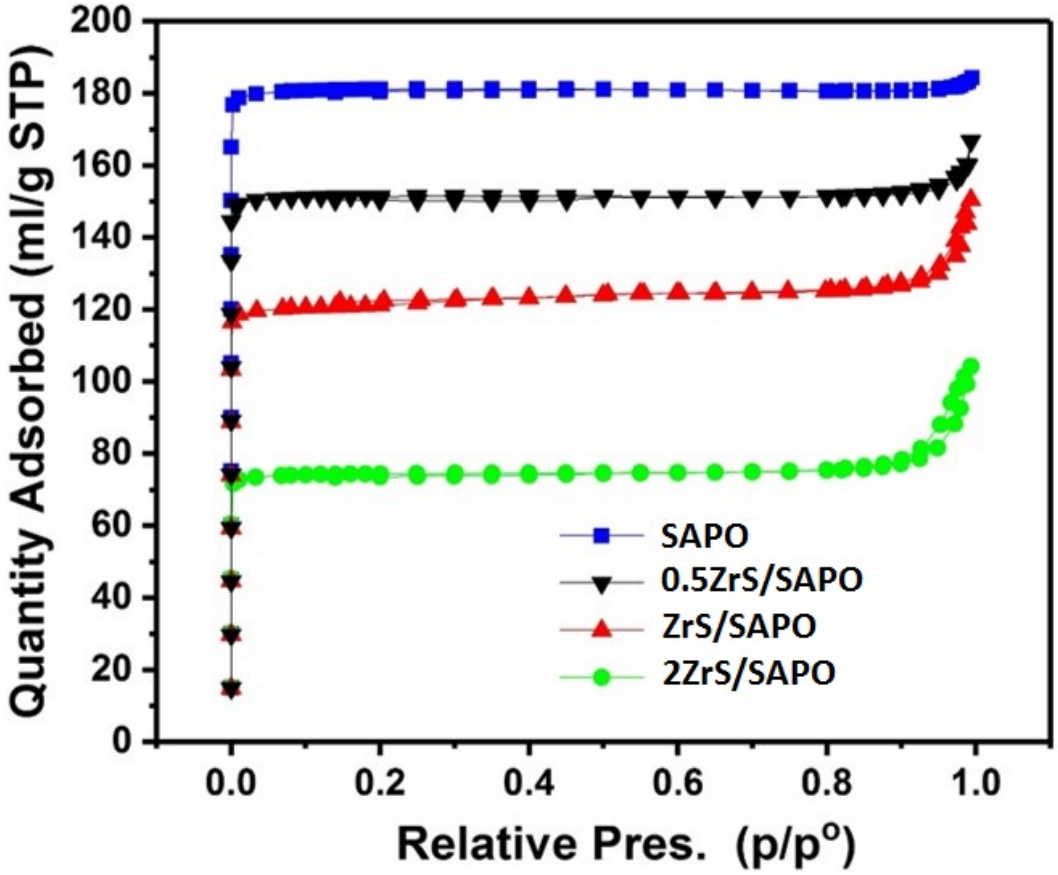

Figure S3. Nitrogen adsorption-desorption isotherms of Zr/SAPO-34 materials.

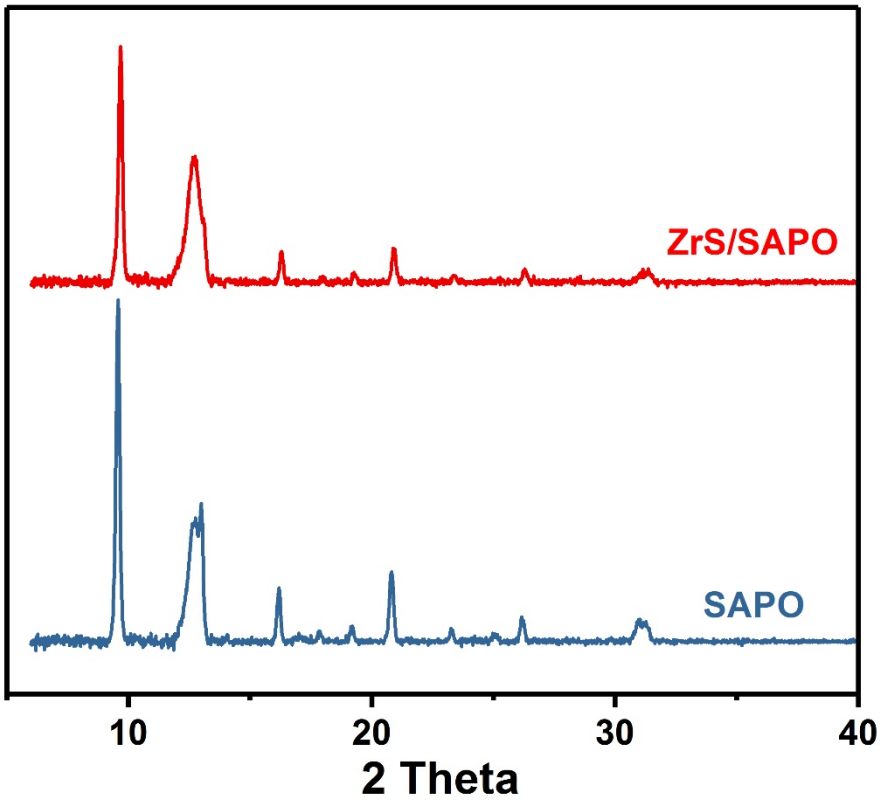

Figure S4. X-Ray diffraction (XRD) patterns of SAPO-34 and Zr/SAPO-34.

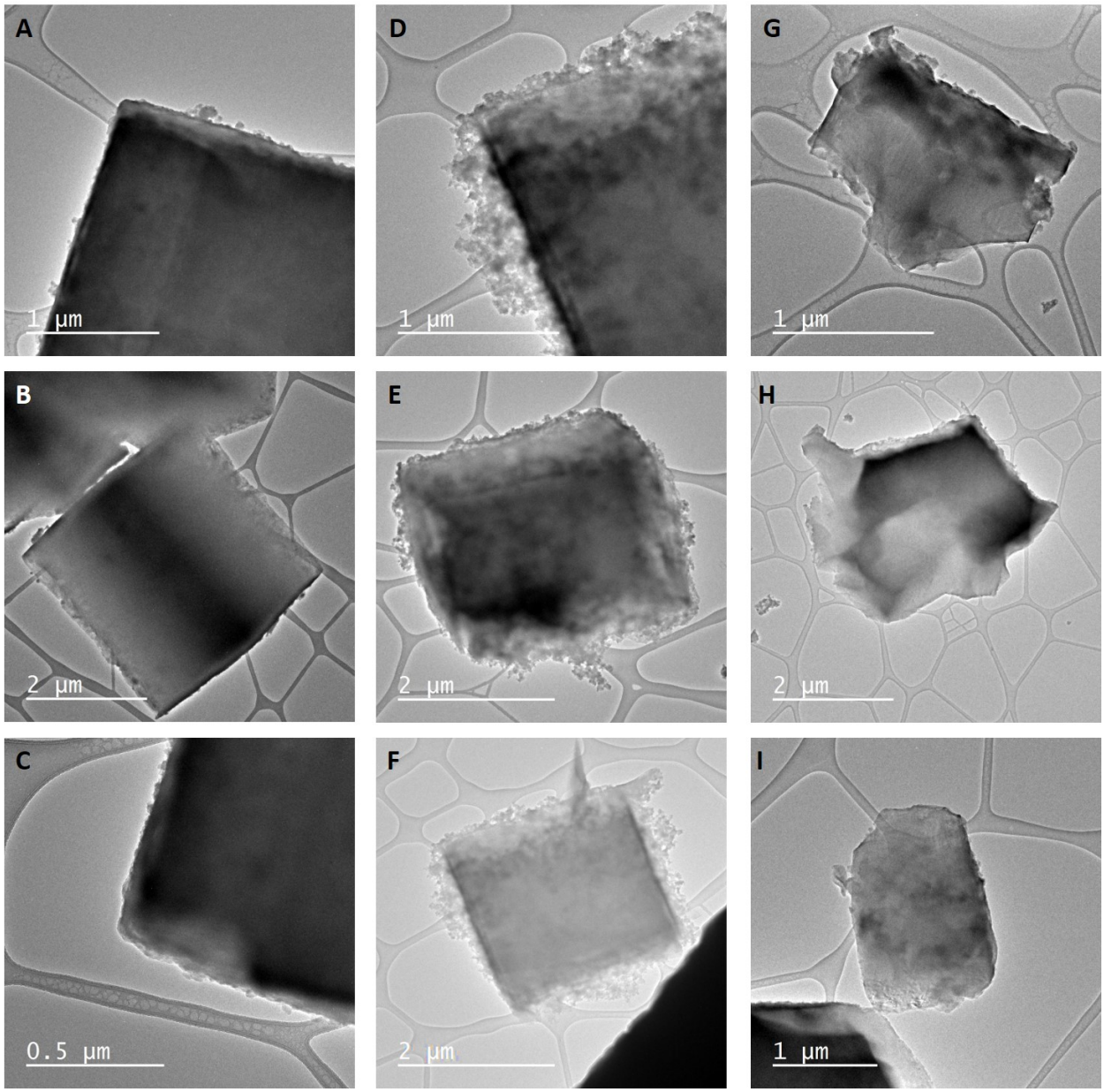

Figure S5. TEM images of the different ZrS loaded SAPO-34 materials. (A, B, C) TEM image of 0.5xZrS/SAPO-34. (D, E, F) TEM images of ZrS/SAPO-34. (G, H, I) TEM image of 2xZrS/SAPO-34.

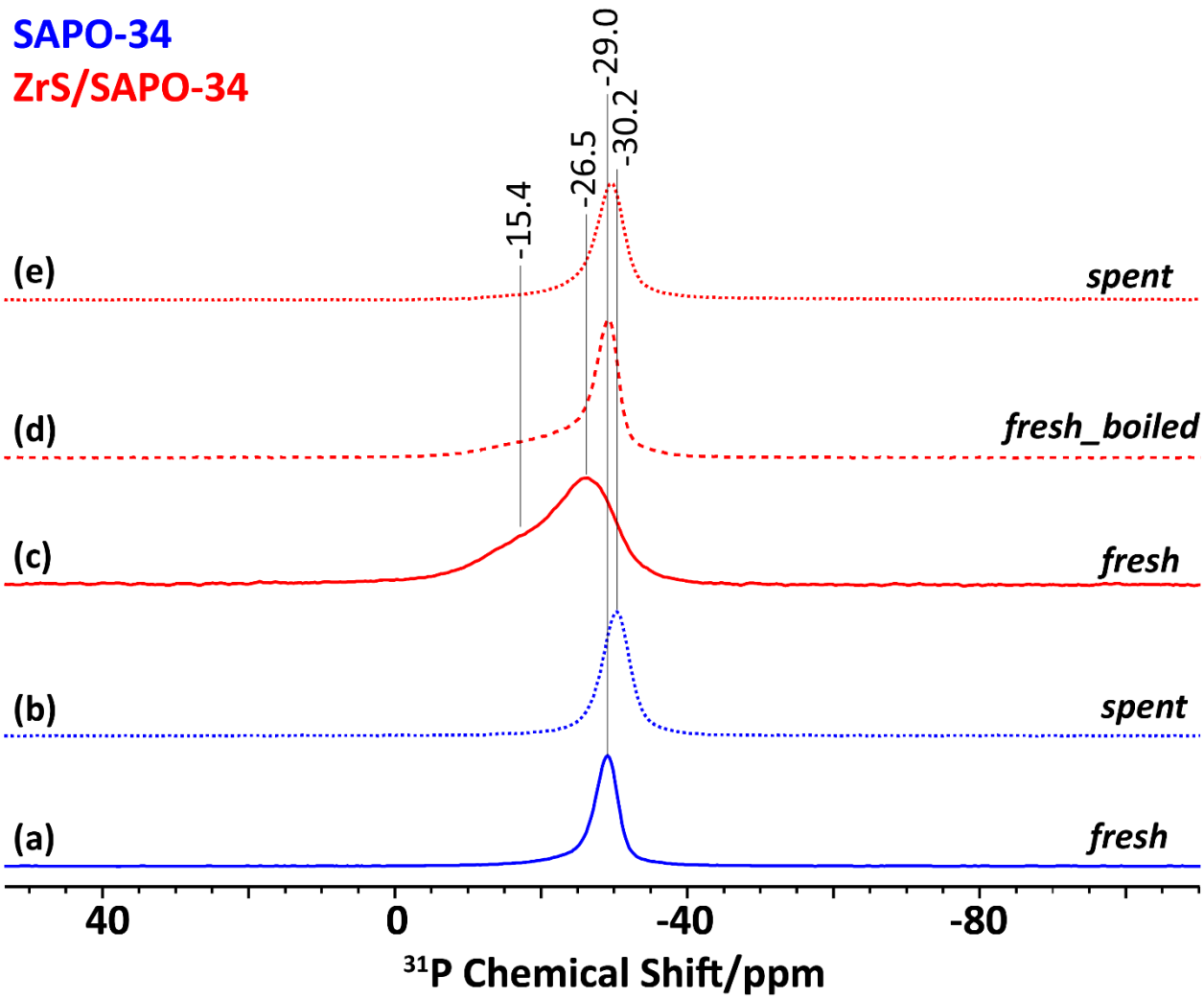

AlPO-phase: -28 to -32 ppm
Aluminum-bonded middle-chain phosphate groups: -26.5 ppm
Free-chain end groups (e.g. pyrophosphates, not bonded to aluminum) : -15.4 ppm

Figure S6. ^{31}P magic angle spinning (MAS, 20KHz) solid-state nuclear magnetic resonance spectra of (a) fresh H-SAPO, (b) post-reacted SAPO, (c) fresh ZrS/SAPO-34, (d) fresh ZrS/SAPO-34 after boiling in water for 12 hours, and (e) post-reacted ZrS/SAPO-34. The slight difference between fresh and spent sample is due to the deposition of coke after the reaction. Post-reacted materials were prepared after the hydrogenation of carbon dioxide over for 50 hours.

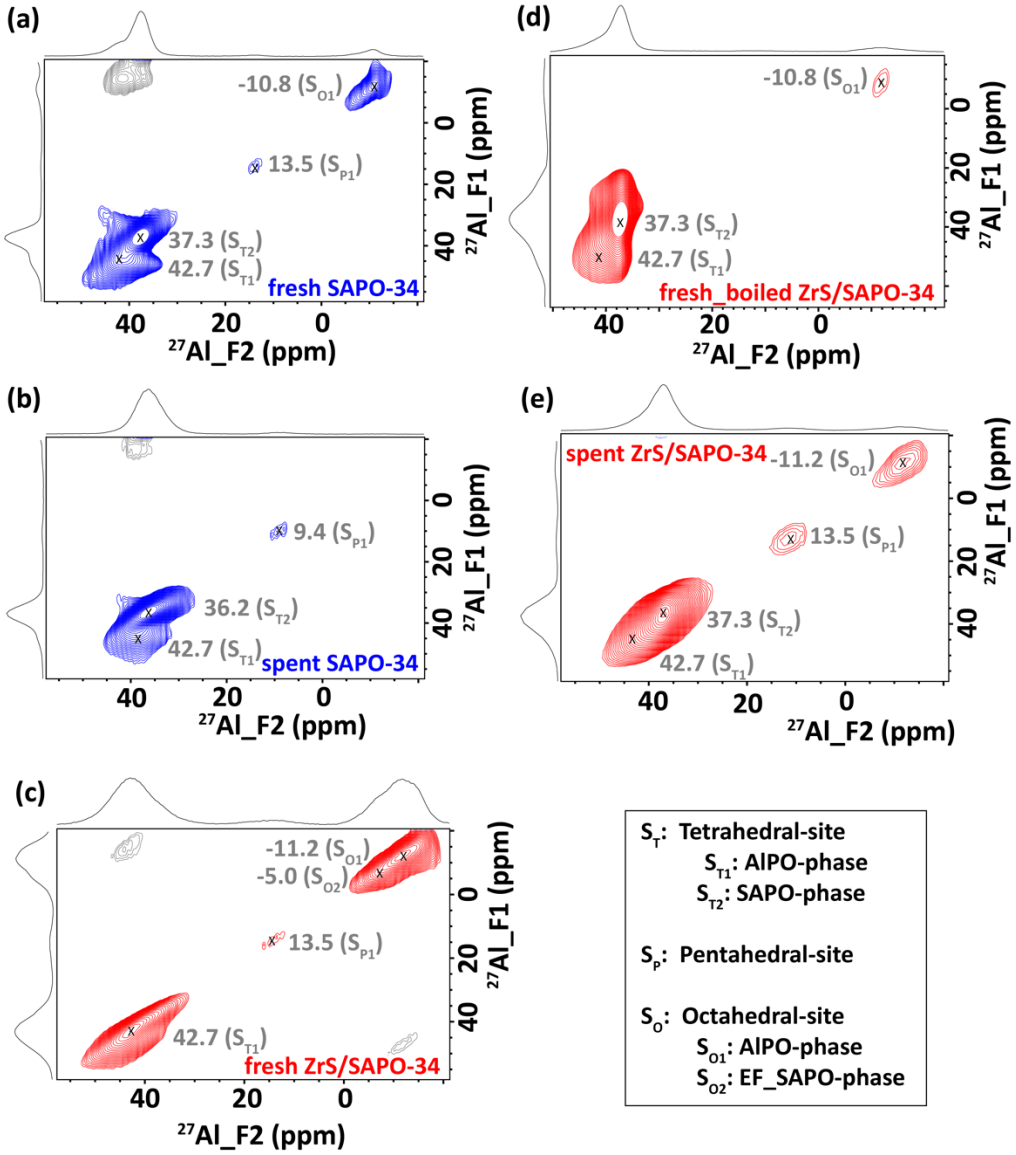

Figure S7. 2D ^{27}Al multiple-quantum (MQ) magic angle spinning (MAS, 20KHz) solid-state nuclear magnetic resonance spectra of (a) fresh H-SAPO, (b) post-reacted SAPO, (c) fresh ZrS/SAPO-34, (d) fresh ZrS/SAPO-34 after boiling in water for 12 hours, and (e) post-reacted ZrS/SAPO-34. Post-reacted materials were prepared after the hydrogenation of carbon dioxide for 50 hours.

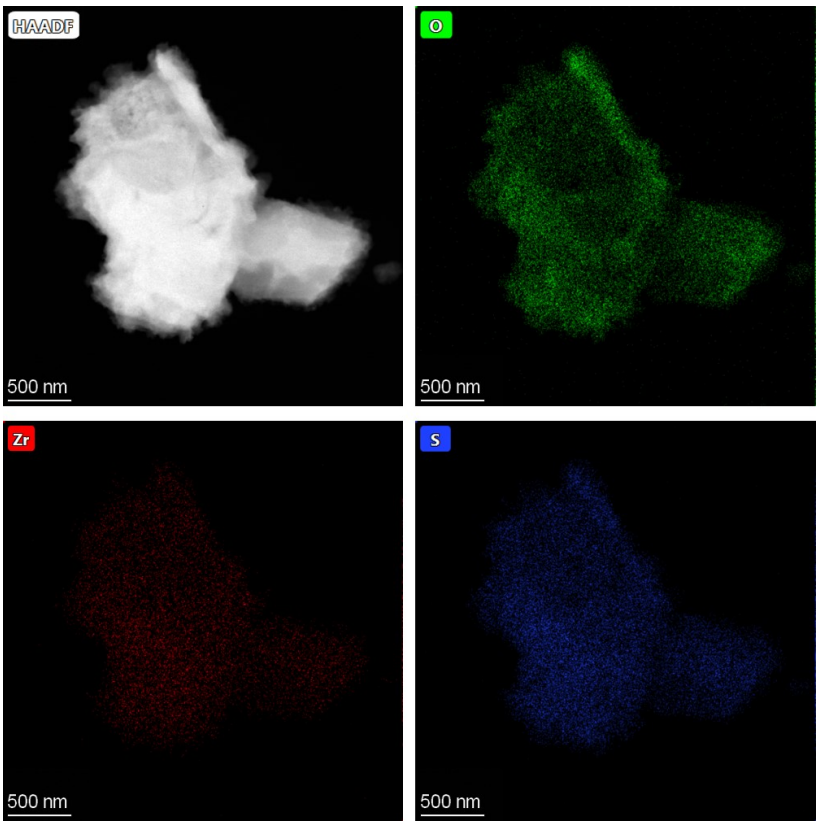

Figure S8. HAADF-STEM image and elemental analysis of the stand-alone ZrS catalyst.

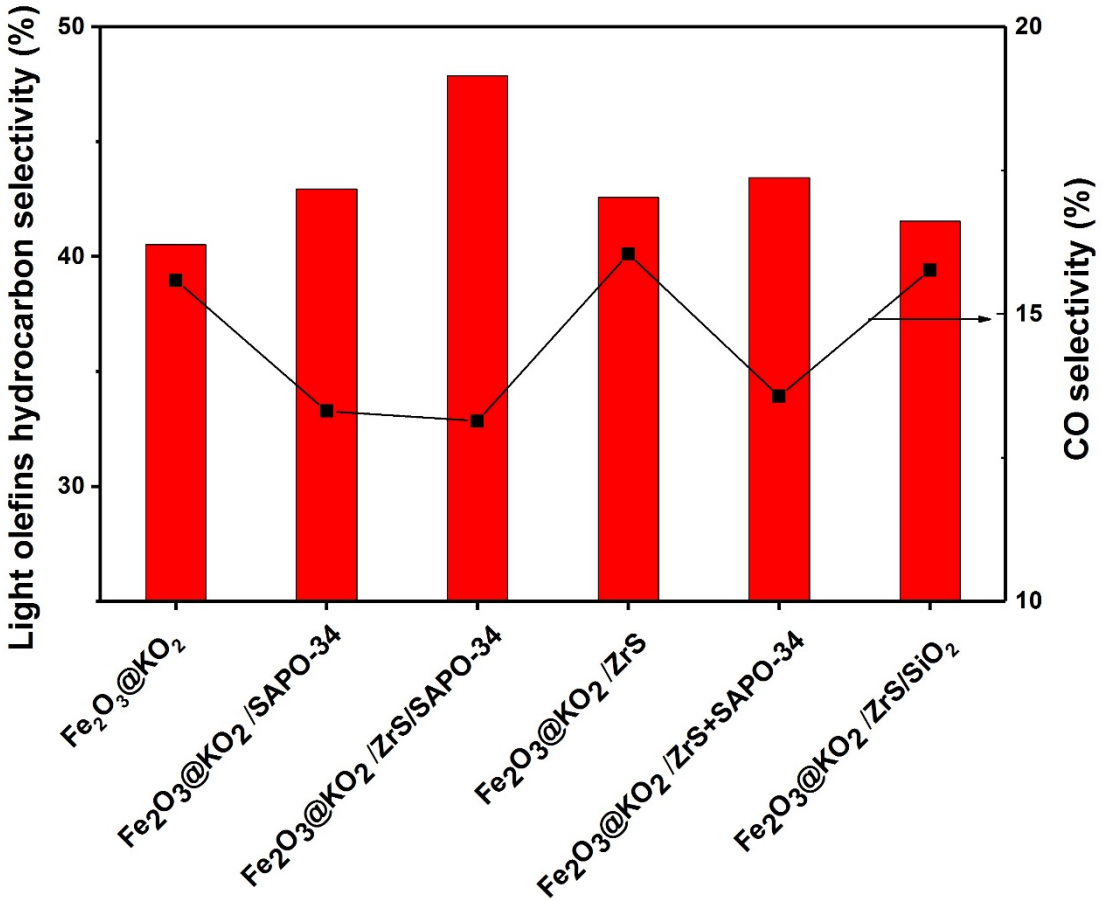

Figure S9. Catalytic performance of the different configurations for the multifunctional materials after a TOS of 50 h. Reaction conditions: 375 ^{0}C, 30 bar, H_2/CO_2 = 3, and 5000 mL·g^{-1}·h^{-1}. ZrS states for bulb ZS, ZrS/SAPO-34 states for ZrS coated SAPO-34, ZrS for physically mixed ZrS and SAPO-34 and ZrS/SiO_2 for ZrS impregnated SiO_2.

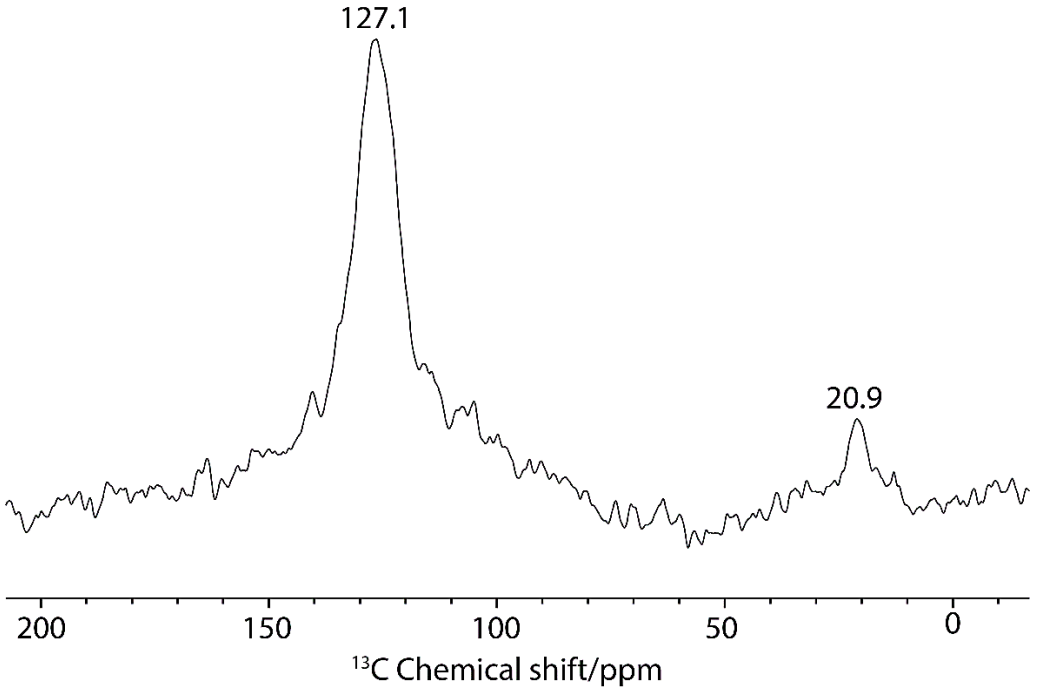

Figure S10. ^{13}C direct excitation MAS solid-state NMR spectra of post-reacted SAPO material trapped organic products after the control reaction involving the mixture of ^{13}CO, ethylene and hydrogen for 6 hours at $375^{0}C$ and 30 bars (MAS= magic angle spinning=20kHz, NS=number of scans=1408, recycle delay=4 seconds).

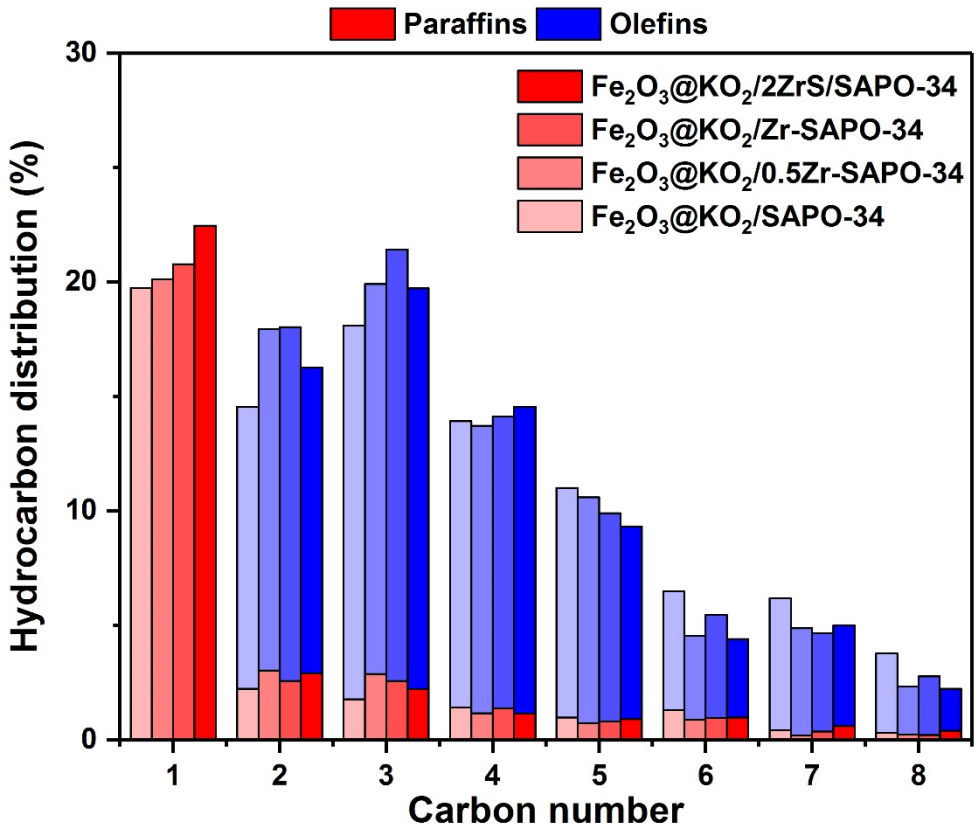

Figure S11. Catalytic performance of the different ZrS loaded SAPO-34 materials after a TOS of 50 h. Reaction conditions: 375 ^{0}C, 30 bar, H_2/CO_2 = 3, and 5000 mL·g−1·h−1.